J Musculoskelet Neuronal Interact 2025; 25(1):1-17

Journal of Musculoskeletal and Neuronal Interactions JMNI

Original Article

Biomechanics of a Drop Landing: Osteogenic Stimulus Measures May Vary

Andrew R. Wilzman[1], Devin T. Wong[2], Karen L. Troy[1]

[1]Department of Biomedical Engineering, Worcester Polytechnic Institute, Worcester, MA, USA;
[2]University of Rochester, Rochester, NY, USA

Abstract

Objectives: Impact exercises are known to increase bone mineral density (BMD) through the biological process of bone remodeling, increasing strength and resistance to fracture. The purpose of this study was to compare several measures that have been used as surrogates for bone impact as a magnitude of its potential to induce bone remodeling. **Methods**: Twenty healthy adults (10 male, 10 female) participated in a biomechanical investigation of how drop height and landing style (bilateral vs. unilateral) affect various estimates of bone remodeling stimuli. These stimuli surrogates include accelerations measured by Inertial Measurement Units (IMUs), ground reaction forces, joint contact forces estimated by musculoskeletal modeling, and tibia strains estimated by finite element modeling. **Results**: Drop height was directly related to stimulus magnitudes, but there was little benefit to drop heights greater than 0.4 m. In contrast, switching from a bilateral to a unilateral landing had a large positive effect. A post-hoc analysis revealed that a linear regression of kinematics and reaction force explained up to 79% of the variance in computationally expensive bone remodeling stimulus measures. **Conclusions**: subject-specific bone strain analysis may not be necessary to understand the magnitude of a bone remodeling stimulus of an exercise.

Keywords: Bone, Computational, Finite Element Method, Osteoporosis, Remodeling

Introduction

To load, but not overload; to use, but not overuse - these are the recommendations offered to those who seek to improve their skeletal strength for a reduced risk of fracture later in life. Osteoporosis is a skeletal disorder defined by a reduction in bone mineral density (BMD) due to old age. This systemic BMD loss results in weak skeletal tissue, and an overall increased risk of bone fracture[1–4]. Osteoporosis affects women at a higher rate than men, with approximately 20% of women and 12% of men across the world[4,5]. A recent large-scale review of Medicare spending data in the United States found a total increase of over $30,000 in spending for patients with bone fractures due to osteoporosis in the first year after fracture[6]. The prevalence of osteoporosis places a significant burden on healthcare spending, but the real impact of the disease is a continuously decreasing capability to maintain independence and quality of life in the aging population.

Osteoporosis is most effectively prevented by optimizing peak bone mass, which occurs during young adulthood[7,8]. Bone tissue is known to adapt to mechanical loading through a mechanism driven by osteocytes that coordinate bone apposition, targeting areas of high strain[8–11]. First proposed by Harold Frost in 1987, the “mechanostat” theory states that bone works to stiffen these areas of high strain to result in a structure optimized for the forces regularly imposed on the skeleton[12]. In a 2003 update, Frost wrote about bone’s ability to sense these forces as a signal and prioritize them based on frequency[13]. Since then, researchers have been eager to study and test the theory by measuring the osteogenic effects of new skeletal loads on bone structure and density, such as introducing new loading by adding jumping to exercise routines[14,15]. Although numerous theoretical models

The authors have no conflict of interest.

Corresponding author: Karen L. Troy, PhD, Departments of Biomedical and Mechanical Engineering, Worcester Polytechnic Institute, 100 Institute Road, Worcester, MA 01609, USA
E-mail: ktroy@wpi.edu

Edited by: G. Lyritis
Accepted 24 September 2024

for the relationship between exercise parameters and bone remodeling have been tested and published, the magnitude of their effects in humans are unknown[16–20].

In 2010, Ahola et al. proposed the Daily Impact Score (DIS) as an accelerometer-based remodeling stimulus[17]. Since then, more computationally intense methods have been developed and tested, particularly using Finite Element (FE) models[21–25]. While models have grown in complexity, it is unclear whether the additional cost of data and computation are justified by a different result. The key input value can be thought of as a theoretical bone remodeling stimulus, with the understanding that the stimulus decays with each repetition yet is cumulative over the time it takes the bone to adapt[20].

In this study, we focused on how to quantify the magnitude of the stimulus, and how a person could voluntarily manipulate this stimulus by modifying their activity or biomechanics. We also investigated how a theoretical bone remodeling stimulus would change, based on the amount and sophistication of the data available. We considered three levels of detail for the applied forces to the skeleton. The simplest measure is based on tibia acceleration, which can be easily captured with low-cost Inertial Measurement Units (IMUs). The next is vertical ground reaction force, whose measurement requires calibrated force platforms or pressure-sensing insoles. The most detailed force metric is an estimate of total joint contact force. This requires three-dimensional motion capture and musculoskeletal modeling to determine and sum the ground reaction force and estimated muscle force vectors. This force could then be applied to an FE model representing the tibia to calculate the bone's strain reaction. The high cost of computation, expert labor, and high-precision measurements across multiple, expensive systems brought us to our final question: are all these systems and data required to understand the magnitude of a theoretical bone remodeling stimulus?

To answer the proposed question, we designed an example bone loading exercise that would optimize bone impact with respect to energy required to complete a task set. Dropping from elevated surfaces was selected as the task, taking advantage of gravity and simplicity. Thus, this study had two goals: (1) to determine the degree to which different landing methods could manipulate theoretical bone remodeling stimulus magnitudes, and (2) to understand the value of added complexity in estimating these stimuli. Our hypotheses for the first goal were that unilateral jump landings would produce higher stimulus magnitudes than bilateral landings and that jump height would be directly related to stimuli. For the second goal we hypothesized that a combination of less detailed inputs can be modeled to predict more detailed stimulus magnitudes.

Methods

Data Collection

Twenty healthy adults (Table 1) were included in the study. Upon consent and meeting inclusion criteria for the study, we recorded their age, height, weight, sex, and musculoskeletal injury history. High resolution peripheral quantitative CT (HRpQCT, XtremeCT I, Scanco, Switzerland) was used to image a standardized 9.01 mm 3D region of each participant's right distal tibia located

Table 1. Participant demographics reported as mean (standard deviation).

	Male (n = 10)	Female (n = 10)
Height (m)	1.784 (0.043)	1.628 (0.051)
Mass (kg)	73.5 (7.5)	55.4 (5.7)
Age (years)	22.1 (2.2)	21.3 (1.3)

Table 2. Participant task set.

Task	Sets x Trials	Instruction
Bilateral Drop	4 x 3	Jump down from 0.2, 0.4, 0.5, and 0.6 m platforms onto force plates with both feet.
Unilateral Drop	4 x 2	Jump down from 0.2, 0.4, 0.5, and 0.6 m platforms, landing on only the right foot.

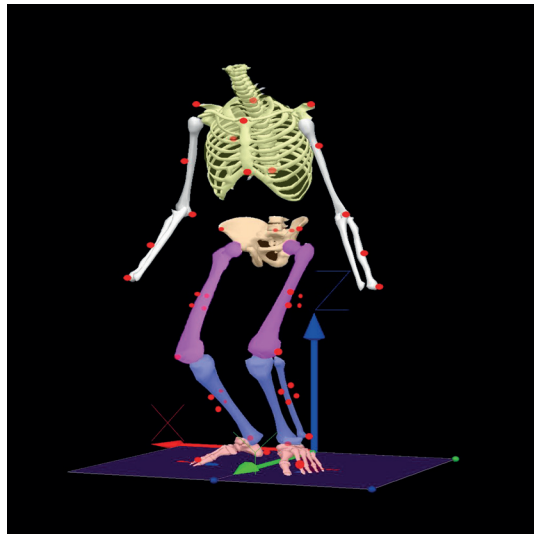

Figure 1. The modified plug-in gait marker set was supported by lower extremity clusters for orientation tracking without medial markers.

Table 3. Outcome variables tested here, ranked by complexity.

Outcome	Abbreviation	Units	Complexity
Daily Impact Score	DIS	--	1
Tibia Acceleration FFT Integral	IMU_FFT	m/s^3	1
Maximum Ground Reaction Force	RXF	BW	2
Maximum Ground Reaction Force Rate	RXF_R	BW/s	2
Ground Reaction Force FFT Integral	RXF_FFT	BW/s	2
Maximum Joint Contact Force	JCF	BW	3
Maximum Joint Contact Force Rate	JCF_R	BW/s	3
Joint Contact Force FFT Integral	JCF_FFT	BW/s	3
FE Tibia Compressive Strain, due to Ground Reaction Force	RXF_FE	mm	4
FE Tibia Compressive Strain, due to Ground Reaction Force, FFT Integral	RXF_FE_FFT	mm/s	4
FE Tibia Compressive Strain Magnitude * Rate, due to Ground Reaction Force	RXF_SMR	mm^2/s	4
FE Tibia Compressive Strain, due to Joint Contact Force	JCF_FE	mm	5
FE Tibia Compressive Strain, due to Joint Contact Force, FFT Integral	JCF_FE_FFT	mm/s	5
FE Tibia Compressive Strain Magnitude * Rate, due to Joint Contact Force	JCF_SMR	mm^2/s	5

22.5 mm proximal to the distal subchondral plate (82 µm voxel size, 59.4 kV and 900 mA, effective radiation dose: 0.3 mSv).

For the experiment, each participant removed their shoes and had at least five minutes to stretch and warm up before beginning motion tasks. Participants were also allowed to practice the drop landings at each height before data collection. Forty-one passive reflective markers were applied to the body using a modified plug-in gait marker set with extra clusters on the thighs and shanks (Figure 1)[26]. Marker trajectories were measured using a ten-camera motion capture system (100 Hz, Vicon Motion Systems Ltd, UK), reaction forces with two six-axis force plates (1000 Hz, AMTI, Watertown, MA), and tibial acceleration with a dual IMU/EMG system adhered to the tibialis anterior (1000 Hz, Delsys Trigno Avanti, Delsys Inc., Natick, MA). The tasks were completed in the order shown in Table 2.

Data Processing

The measured trajectory of each marker was filtered through a fourth order low-pass Butterworth filter with a cutoff frequency of 6 Hz, while the force plate timeseries was filtered using the same with a 300 Hz cutoff. The outcomes were designed to represent an osteogenic stimulus measure from each participant during the measured task. They were divided into four sections, with increasing degrees of complexity of data and/or invasiveness to the person to collect. To model the contributions of both loading magnitude and rate[20,27], each force related outcome included a product of magnitude and rate[24], or the first half of the integral of the timeseries' Fast Fourier Transform (FFT)[20,24]. The total pool of outcomes is detailed in Table 3.

Tibia Acceleration

A Delsys Trigno Avanti sensor affixed to the right anterior shank was used to measure tibial acceleration (sampling rate: 1000 Hz), and the data were passed through a 20 Hz, fourth order low-pass Butterworth filter. The maximum acceleration magnitude was binned according to the Daily Impact Score (DIS)[17]. The integral of the Fourier transform was also recorded (IMU FFT).

Ground Reaction Force

Ground reaction force was measured using a 1000 Hz, 6-axis force plate embedded into the landing surface. The resulting data included maximum reaction force (RXF), maximum force rate (RXF_R), and the integral of the Fourier transform (RXF_FFT).

Joint Contact Force

The motion capture data were exported to Visual 3D (C-Motion, Gaithersburg, MD) to model body segments and calculate inverse kinematics and dynamics. We filtered the data again through a fourth-order, 6 Hz low-pass Butterworth filter and exported the result to OpenSim 4.4[28,29], using model Gait 2392 as the basis for our calculations[30]. After model scaling, static optimization was used to estimate lower extremity muscle forces for each trial. Finally, total joint contact force at the ankle was calculated by summing the forces of all muscles crossing the ankle joint along with the net joint force calculated from inverse dynamics. The maximum ankle joint contact force (JCF), maximum force application rate (JCF_R), and integral of the Fourier transform (JCF_FFT) were recorded.

Tibia Compressive Strain

Subject-specific FE models of a 9.01 mm section of the distal tibia were created from HRpQCT images. A Scanco built-in FE solver was used with a single tissue model (E = 10 GPa, Poisson's ratio = 0.3) with linear-elastic, isotropic material properties[31,32] to estimate axial tibia stiffness (in N/mm) under platen compression. Reaction strain (RXF_FE) and contact strain (JCF_FE) were calculated by dividing RXF and JCF, respectively, by axial tibia stiffness. The time series were also analyzed to extract maximum tibial strain rates[24]. This produced the last outcomes: reaction and contact strain magnitude * rates (SMR) and integral Fourier transforms (RXF_SMR, JCF_SMR, RXF_FE_FFT, JCF_FE_FFT). Among these, JCF_SMR is considered to be the most accurate metric, since it incorporates subject-specific anatomy, and the most relevant aspects of the mechanical signal applied to the tibia.

Statistical Analysis

Pearson correlations between outcome variables were calculated to assess relationships. We expected the outcomes to be highly correlated within each complexity group; however, the correlations outside of these groups shed light on how the different types of measurement produce different estimates of a bone adaptation stimulus. We also analyzed correlations between key kinematic predictor variables: joint angle at contact and joint range of motion for the hip, knee, and ankle of the analyzed leg.

The first hypothesis of the study was that unilateral jump landings would produce higher stimulus magnitudes than bilateral landings. A paired t-test was used to assess the differences between each stimulus metric between landing conditions. The alpha significance threshold was set to 0.05 and we corrected false discovery rate due to multiple comparisons by using the Holm-Bonferroni method[33,34].

Jump height was hypothesized to be directly related to stimulus magnitudes. To test this, jump height, landing limbs, and the interaction of two were regressed with each outcome in a k-fold cross validation scheme (k = 5). Significance was assessed via the mean testing p-value of each model. As before, we corrected multiple comparisons using the Holm-Bonferroni method.

The third hypothesis was that a combination of less detailed inputs could be modeled to predict more detailed stimulus magnitudes. To test this, the Least Absolute Shrinkage and Selection Operator (LASSO) was employed to choose predictor variables in the regression for each outcome. The pool of possible predictors was restricted to variables with lower complexity, including the kinematic predictors as a baseline. If height and number of landing legs were deemed significant, these were added as predictors. Kinematic predictors were included due to known relationships between range of motion and contact angle and loading rates[35]. The training data were normalized to a z-score as a preprocessing step and each feature's scalar was saved to be applied on the predictors of the testing set. Our hypothesis was tested across each outcome variable using the average model's prediction on a held-out test set after a k-fold cross-validation procedure (k = 5) on a training set. The p-values were obtained from the test results. As before, we corrected false discovery rate due to multiple comparisons using the Holm-Bonferroni method. Overall model significance was measured using an F-statistic, and fit was assessed via the average coefficient of determination (R^2) and Mean Absolute Error (MAE) on the testing sets. If a model was deemed significant, each coefficient's significance was assessed using a t-statistic.

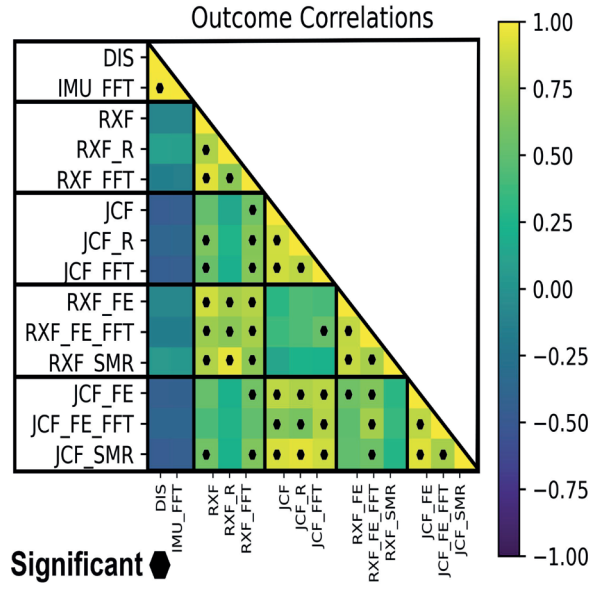

Figure 2. Correlations between key outcomes reveal expected within-group correlations but an unexpected inverse relationship between force and IMU-based measures.

Results

Pearson correlations of outcomes within the same complexity group were generally high and significant. The IMU-related outcomes showed prominent disagreement, albeit with insignificant correlations, with measured reaction and joint contact forces (Figure 2). Correlations between reaction (RXF) and contact forces (JCF) were slight and sparsely significant. RXF_FE_FFT was most closely related to the JCF variables.

Hypothesis 1: Unilateral vs. bilateral

As expected, unilateral jump landings produced significantly higher stimulus magnitudes than bilateral

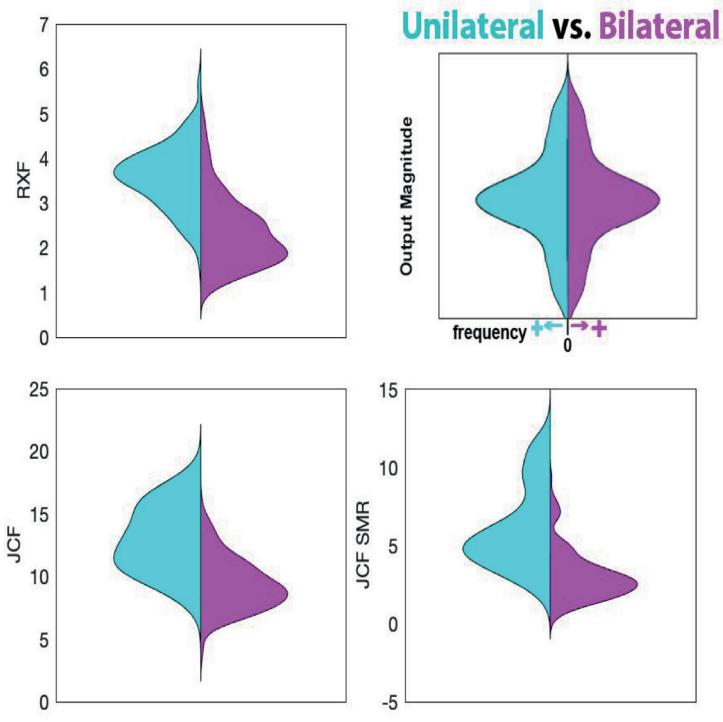

Figure 3. Each graph shows a histogram that represents the frequency (x axes) of each output magnitude (y axes), mirrored across unilateral (left) and bilateral landings (right). Unilateral trials consistently achieved higher outcome values. Each comparison shown was significant with an alpha threshold of 0.05 and Holm-Bonferroni correction for multiple comparisons.

Table 4. Comparison of the relative influence of drop height and landing limbs on select outcomes. Bolded models were significant with $p < 0.05$ and Holm-Bonferroni correction.

Outcome	Complexity Group	Coefficients (β)		p-value	Model R^2	Model p-value
RXF	2	**Drop Height**	**2.59**	**0.001**	0.472	**<0.001**
		Landing Limbs	**-1.03**	**<0.001**		
		Interaction	-0.45	0.427		
JCF	3	Drop Height	**12.43**	**<0.001**	0.440	**<0.001**
		Landing Limbs	**-1.60**	**0.015**		
		Interaction	**-4.24**	**0.015**		
JCF_SMR	5	**Drop Height**	**10.72**	**<0.001**	0.372	**<0.001**
		Landing Limbs	**-1.20**	**0.035**		
		Interaction	**-3.83**	**0.021**		

landings. While the daily impact score and IMU FFT outcomes were significantly different between the landing groups, the relationship was reversed, as suggested by the correlation analysis. These data were removed from the remaining computational analyses.

Hypothesis 2: Drop Height

Across the board, 0.2 m height produced significantly lower stimulus magnitudes than 0.5 and 0.6 m groups. Fewer outcomes were significantly different in comparison

Table 5. Average testing results of linear regression on FE_FFT variables using jump height (H), landing limbs (L), and sex (S). The MAE is reported in standardized units (SD).

Outcome	Predictor(s)			β p-value(s)			MAE (SD)	R^2	Model p-value
RXF_FE_FFT	H			**<0.001**			0.77	0.02	0.492
JCF_FE_FFT	H			**<0.001**			0.73	0.02	0.434
RXF_FE_FFT	L			**<0.001**			0.64	0.31	**<0.001**
JCF_FE_FFT	L			**<0.001**			0.67	0.18	**0.012**
RXF_FE_FFT	S			**<0.001**			0.75	0.14	0.205
JCF_FE_FFT	S			**<0.001**			0.67	0.18	**0.009**
RXF_FE_FFT	H	L	H*L	**0.004**	**<0.001**	0.572	0.62	0.35	**0.003**
JCF_FE_FFT	H	L	H*L	**0.034**	**0.003**	0.480	0.62	0.24	**0.006**
RXF_FE_FFT	H	S	H*S	**<0.001**	0.345	0.560	0.74	0.16	0.051
JCF_FE_FFT	H	S	H*S	**0.009**	0.100	0.728	0.66	0.16	**0.012**
RXF_FE_FFT	L	S	L*S	**<0.001**	**0.001**	0.190	0.54	0.51	**<0.001**
JCF_FE_FFT	L	S	L*S	**<0.001**	**0.028**	0.202	0.57	0.40	**<0.001**

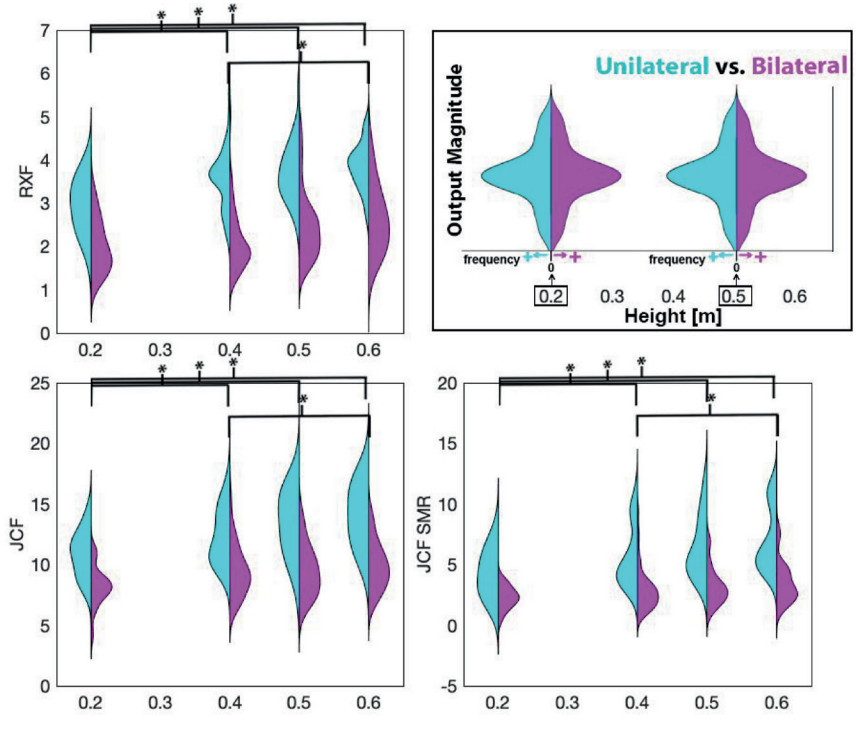

Figure 4. Generally, jump height was found to significantly increase each outcome between 0.2 m and each of the greater heights. In some cases, 0.5 m and/or 0.6 m significantly increased outcomes over 0.4 m. Each histogram represents the frequency of outputs, mirrored with respect to unilateral and bilateral landings. Significant comparisons are denoted above.

with heights at 0.4 m and higher (Figure 4). Each outcome was then regressed with jump height, landing limbs, and the interaction between them to determine the height's relative influence. Height remained a significant predictor in many cases (Table 4).

In further post-hoc analyses, sex was included as a numeric variable with 0 and 1 representing female and male, respectively. Sex was found to be significant when

predicting RXF_FE_FFT and JCF_FE_FFT, the only outcomes that combine a summation of force magnitude over its entire frequency spectrum. In each case, females generated higher outcome values than males. In a univariate analysis, sex explained an average of 14% of the variance in RXF_FE_FFT and 18% of the variance in JCF_FE_FFT across the k-fold validation scheme.

When height and landing limbs were included separately in multivariate regressions along with sex and an interaction term (X_1*X_2), the coefficient for sex was only significant when predicting RXF_FE_FFT and JCF_FE_FFT while the interaction term never reached significance. Alone, number of landing limbs explained 31% and 18% of the variance of RXF_FE_FFT and JCF_FE_FFT, respectively. When sex was included, these increased to 51% and 40%, respectively. Jump height was always a significant predictor yet failed to reach significance alone (Table 5).

Hypothesis 3: Linear Modeling

Because height, number of landing legs, and sex affected outcomes, these were included as predictors in the LASSO regression models. In contrast, interaction terms and IMU-based data were omitted due to their overall lack of significance. The first set included only kinematic variables as predictors for baseline models (Table 6). For complexity groups 2 and higher, the result of the outcomes in all lower complexity groups were included in the predictor pool (Table 7). Many models were found to be significant after a Holm-Bonferroni correction, some exceptions being rate-dependent outcomes calculated with reaction forces predicted by kinematics only.

The LASSO models that predicted outcomes without FE showed marginal improvement over its counterpart that only includes kinematics. These models tended to assign large coefficients to joint reaction and contact forces compared to the other possible predictor variables. To compare how these FE outcomes could be predicted without musculoskeletal modeling (required to determine joint contact forces), JCF data were removed for new models. When JCF is included, slight improvements are seen in reaction force FE outcomes, while rate-dependent JCF FE (JCF_FE_FFT and JCF_SMR) outcomes greatly improved (Table 8).

Table 6. Testing results for LASSO regression on each outcome using kinematics, height, landing legs, and sex. Significant models are **bolded**, all else are in *italics*.

Outcome	Complexity	MAE (σ)	R^2
RXF	2	**0.53**	**0.53**
RXF_R		*0.68*	*0.08*
RXF_FFT		**0.39**	**0.74**
JCF	3	**0.49**	**0.64**
JCF_R		**0.47**	**0.70**
JCF_FFT		**0.41**	**0.72**
RXF_FE	4	**0.59**	**0.39**
RXF_FE_FFT		*0.64*	*0.34*
RXF_SMR		*0.61*	*0.10*
JCF_FE	5	**0.39**	**0.74**
JCF_FE_FFT		**0.51**	**0.47**
JCF_SMR		**0.41**	**0.72**

Discussion

The positive effect that jumping exercises have on bone mineral density are clear in multiple intervention studies[36–39]. From the results of this computational analysis, we would expect to see higher increases in BMD in participants who drop unilaterally, and from heights of at least 0.4 m. Our findings are consistent with a 2018 review article that concluded ground reaction forces should exceed 3.5 * BW to be effective

Table 7. Testing results for LASSO regression on each outcome using lower complexity outcomes, kinematics, height, landing legs, and sex. The difference in comparison to kinematic models (Table 6) is shown to the right of each metric. All models were found to be significant after Holm-Bonferroni correction.

Outcome	MAE (σ)	Difference	R^2	Difference
JCF	0.45	-8.9%	0.72	+11.1%
JCF_R	0.38	-18.9%	0.78	+12.0%
JCF_FFT	0.40	-4.3%	0.75	+4.1%
RXF_FE	0.30	-43.6%	0.88	+66.8%
RXF_FE_FFT	0.45	-29.9%	0.67	+95.7%
RXF_SMR	0.18	-70.6%	0.93	+832%
JCF_FE	0.36	-26.7%	0.82	+27.6%
JCF_FE_FFT	0.37	-4.2%	0.79	+6.4%
JCF_SMR	0.19	-58.5%	0.94	+34.7%

Table 8. Testing results for LASSO regression on JCF_FE outcomes show improved performance while RXF_FE predictions only slightly improve when adding estimated contact force predictors.

Outcome	Without JCF data		With JCF data		Difference when JCF is added	
	MAE (SD)	R^2	MAE (SD)	R^2	MAE (SD)	R^2
RXF_FE	0.34	0.83	0.30	0.88	-11.8%	+6.0%
RXF_FE_FFT	0.45	0.67	0.43	0.72	-4.4%	+7.5%
RXF_SMR	0.19	0.92	0.18	0.93	-5.3%	+1.1%
JCF_FE	0.38	0.75	0.36	0.82	-5.3%	+9.3%
JCF_FE_FFT	0.51	0.48	0.37	0.79	-27.5%	+64.6%
JCF_SMR	0.38	0.78	0.19	0.94	-50.0%	+20.5%

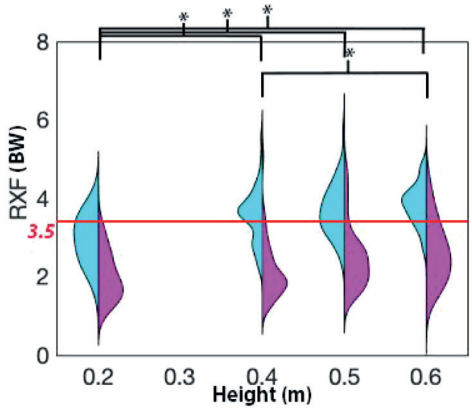

Figure 5. Reaction forces (RXF) above 3.5 BW are seen in unilateral landings (blue) across the board, but only for heights above 0.4 m in bilateral (magenta) landings.

in increasing BMD through exercise intervention[38] (Figure 5). Our study adds to this understanding by demonstrating *how* one can modify a drop jump to achieve a stimulus of this magnitude. The increased stimulus values that we observed during unilateral tasks agrees with an understanding that humans meet them with higher joint stiffness than bilateral tasks[40].

There are many more factors that influence these metrics. For example, one recent study found that a cue to land quietly can immediately reduce ground reaction force rates in runners[41]. In addition, females have been found to use less hip and knee range of motion during unilateral landings, contributing to higher energy absorption at the ankle[42]. Our observation that females had significantly higher values of RXF_FE_FFT and JCF_FE_FFT supports the notion that females may land more stiffly (and with more high-frequency components) than males. It may also indicate differences in bone size and morphology between men and women, though other FE related outcomes did not show a sex effect. We recommend further studies to investigate how landing cues can manipulate these outcomes differently between females and males[43].

The IMU data showed a clear opposition to the remainder of the outcomes. We speculate that this highlights a need for clear and robust fixation methods of IMU placement. Here, the IMU data were recorded on the same device as EMG data, which requires placement on a point of a muscle (the tibialis anterior) that maximizes cross-sectional area and minimizes skin occlusion distance. These devices were then subject to soft tissue artifacts not normally seen when applying standalone IMU devices over fixed to bony landmarks (e.g. at the distal tibia[44]). The magnitude of these artifacts is almost certainly affected by the stiffness of the underlying tissues. Passive reflective markers for motion capture also suffer from noise attributed to soft tissue artifacts. Although lowpass filters are employed to counteract these effects, the noise still inhibits our ability to capture their true movement.

When the linear models were restricted to kinematic variables, 64-72% of variance in JCF outcomes could be predicted. However, when the same predictor pool was tasked to model the JCF_FE_FFT outcome it failed to reach an R^2 greater than 50%. Similarly, RXF outcomes were not well modeled by the kinematics. Therefore, ground reaction force data should be measured to reliably predict the magnitude of an assumed osteogenic stimulus, highlighted by the success of unrestricted LASSO models tasked to model FE outcomes (Tables 6 and 7).

This analysis included several metrics that are not typically available outside research settings but that we assumed were good measures of osteogenic stimulus based on the literature. We hypothesized that a combination of less detailed inputs could be modeled to predict more detailed stimulus metrics. The LASSO models explained 67% of the variance in joint contact force data if only kinematics and ground reaction forces were known. Once lower complexity outcomes were included as possible predictors, the model increased in accuracy with 79-94% of the variance explained in JCF_FE- outcomes. This could be explained by the inclusion

of the forces that were used to estimate the tibia strain via FE estimated stiffness. Analysis of the coefficients chosen within these linear models revealed a high degree of importance in using reaction forces and musculoskeletal modeling to predict the FE outcomes.

We expected that outcomes within the same complexity group would be highly correlated, and we attribute this correlation to measurements being derived from common means (by device and/or software). Correlations diminished outside of these groups, but the relationships that endured provided enough information to create linear models that predict FE outcomes without the need for CT imaging or any explicit FE modeling. So, peak bone strains may be effectively estimated in musculoskeletal modeling software without FE solvers or bone density measurements. We speculate that this was mainly because the present group of young adult participants had relatively healthy and somewhat homogeneous tibiae. It is still important to account for individual bone strength when estimating osteogenic stimulus in other populations, given the differences in bone stiffness and architecture associated with aging and disease[2,45].

The first limitation of this study begins with the participant pool, which includes only healthy, mostly athletic, college students. Most of the participants were familiar with box jumps and landing strategies. A few participants were less likely to fully drop from the heights during unilateral tasks, using a partial "stepping" method instead of falling from the entire height of the box. However, this highlights the real variation of task understanding when a person is asked to drop from a height onto one leg at a time. In the future, the "step down" version of this exercise could be completed using a handrail for balance, making it potentially suitable for many age and ability groups.

Another limitation of this study included the assumptions made to calculate the muscle force time series required to estimate joint contact forces. In OpenSim, static optimization was used for this, which may be less sophisticated than computed muscle control that takes time dynamics into account[46]. While these may have resulted in slightly different results, the high accelerations of the drop landing caused too much noise in computed muscle control results to be reliable.

Finally, the FE outcomes were based on a standard, platen compressive finite element solver within Scanco's XtremeCT software. The solver assumes that the material properties are linear-elastic and homogeneous and does not take bending stress into account[47,48]. These limitations may act together to decrease the validity of the strain metrics with respect to reality. However, the comparisons between the data remain valid through the standardization of protocol and use of subject-specific information.

Conclusions

Unilateral drop landings significantly increase a theoretical bone remodeling stimulus compared to bilateral landings. Additionally, there may be little benefit to jumping from heights above 0.4 m when examining bone remodeling stimulus. Finally, a post-hoc analysis revealed that females may incur more bone tissue damage during drop landing tasks than males.

The only measurement tool studied here that is practical for use outside of controlled laboratory settings is the IMU. However, outcomes reliant on IMU data showed the opposite effect and should be interpreted with caution. A reader should inquire about the placement of the IMU and whether soft tissue artifacts pose a risk to the integrity of the data. Furthermore, we only consider the DIS developed by Ahola et al. in 2010[17]. Since then, more sophisticated methods have been studied and developed to process IMU data for biomechanics research.

Finally, within a homogenous group, a bone remodeling stimulus can be accurately predicted through a combination of 3D motion capture, accurate ground reaction forces, and musculoskeletal modeling. While this is still a complex process, it may negate the need to use quantitative CT imaging and FE modeling to estimate a bone's strain reaction due to a jump landing. The degree to which these theoretical remodeling stimulus calculations predict actual bone remodeling is yet to be prospectively tested in humans. These data and methods presented here make such future predictions possible.

Ethics approval

The study was approved by the Worcester Polytechnic Institute (IRB HHS #00007374, protocol IRB-19-0683).

Consent to participate

Written informed consent was obtained from all individual participants included in the study.

Funding

The authors acknowledge the Research Experiences for Undergraduates (REU) funding through the US National Science Foundation (NSF Award #2150076) for the opportunity to collaborate with undergraduate researcher Devin Wong.

Acknowledgements

The authors would like to acknowledge Julia Nicolescu, Logan Gaudette, Elizabeth Bowman, and Madalyn Hague for their assistance in data collection and processing, Christopher Gens for his work in data processing, and Christopher Nycz for his support in motion capture data collection.

References

1. Bouxsein ML, Eastell R, Lui LY, Wu LA, de Papp AE, Grauer A, et al. Change in Bone Density and Reduction in Fracture Risk: A Meta-Regression of Published Trials. Journal of Bone and Mineral Research. 2019 Apr 1;34(4):632–42.
2. Szulc P, Dufour AB, Hannan MT, et al. Fracture risk based on high-resolution peripheral quantitative computed

tomography measures does not vary with age in older adults-the bone microarchitecture international consortium prospective cohort study. J Bone Miner Res 2024;39(5):561-570
3. Lewiecki EM. Osteoporosis: Clinical Evaluation. Feingold KR, Anawalt B, Blackman MR, editors. South Dartmouth, MA: MDText.com, Inc.; 2021.
4. Clynes MA, Harvey NC, Curtis EM, Fuggle NR, Dennison EM, Cooper C. The epidemiology of osteoporosis. Br Med Bull 2020;133(1):105-117.
5. Salari N, Ghasemi H, Mohammadi L, Behzadi M hasan, Rabieenia E, Shohaimi S, et al. The global prevalence of osteoporosis in the world: a comprehensive systematic review and meta-analysis. J Orthop Surg Res 2021;16(1):609.
6. Williams SA, Daigle SG, Weiss R, Wang Y, Arora T, Curtis JR. Economic Burden of Osteoporosis-Related Fractures in the US Medicare Population. Annals of Pharmacotherapy 2021;55(7):821–9.
7. Heaney RP, Abrams S, Dawson-Hughes B, Looker A, Looker A, Marcus R, et al. Peak Bone Mass. Osteoporosis International 2001;11(12):985–1009.
8. Troy KL, Mancuso ME, Butler TA, Johnson JE. Exercise Early and Often: Effects of Physical Activity and Exercise on Women's Bone Health. Int J Environ Res Public Health 2018;15(5):878.
9. Burr DB, Robling AG, Turner CH. Effects of biomechanical stress on bones in animals. Bone 2002;30(5):781–6.
10. Mori S, Burr DB. Increased intracortical remodeling following fatigue damage. Bone 1993;14(2):103–9.
11. Burr DB, Martin RB, Schaffler MB, Radin EL. Bone remodeling in response to in vivo fatigue microdamage. J Biomech 1985;18(3):189–200.
12. Frost HM. Bone "mass" and the "mechanostat": A proposal. Anat Rec 1987;219(1):1–9.
13. Frost HM. Bone's mechanostat: A 2003 update. Anat Rec A Discov Mol Cell Evol Biol 2003;275A(2):1081–101.
14. Vasto S, Amato A, Proia P, Caldarella R, Cortis C, Baldassano S. Dare to jump: The effect of the new high impact activity SuperJump on bone remodeling. A new tool to maintain fitness during COVID-19 home confinement. Biol Sport 2021;39(4):1011–9.
15. Zhao R, Zhao M, Zhang L. Efficiency of jumping exercise in improving bone mineral density among premenopausal women: a meta-analysis. Sports Med 2014;44(10):1393-402.
16. Carter DR, Orr TE. Skeletal development and bone functional adaptation. Journal of Bone and Mineral Research 1992;7(S2):S389–95.
17. Ahola R, Korpelainen R, Vainionpää A, Jämsä T. Daily impact score in long-term acceleration measurements of exercise. J Biomech 2010;43(10):1960–4.
18. Adams DJ, Spirt AA, Brown TD, Fritton SP, Rubin CT, Brand RA. Testing the daily stress stimulus theory of bone adaptation with natural and experimentally controlled strain histories. J Biomech 1997;30(7):671–8.
19. Valdimarsson O, Linden C, Johnell O, Gardsell P, Karlsson MK. Daily physical education in the school curriculum in prepubertal girls during 1 year is followed by an increase in bone mineral accrual and bone width--data from the prospective controlled Malmö pediatric osteoporosis prevention study. Calcif Tissue Int 2006;78(2):65–71.
20. Turner CH. Three rules for bone adaptation to mechanical stimuli. Bone 1998;23(5):399–407.
21. McNamara BP, Prendergast PJ, Taylor D. Prediction of bone adaptation in the ulnar-osteotomized sheep's forelimb using an anatomical finite element model. J Biomed Eng 1992;14(3):209–16.
22. Webster D, Schulte FA, Lambers FM, Kuhn G, Müller R. Strain energy density gradients in bone marrow predict osteoblast and osteoclast activity: A finite element study. J Biomech 2015;48(5):866–74.
23. MacNeil JA, Boyd SK. Bone strength at the distal radius can be estimated from high-resolution peripheral quantitative computed tomography and the finite element method. Bone 2008;42(6):1203–13.
24. Troy KL, Mancuso ME, Johnson JE, Wu Z, Schnitzer TJ, Butler TA. Bone Adaptation in Adult Women Is Related to Loading Dose: A 12-Month Randomized Controlled Trial. J Bone Miner Res 2020;35(7):1300–12.
25. Mancuso ME, Wilzman AR, Murdock KE, Troy KL. Effect of external mechanical stimuli on human bone: a narrative review. Progress in Biomedical Engineering 2022;4(1):012006.
26. McGinley JL, Baker R, Wolfe R, Morris ME. The reliability of three-dimensional kinematic gait measurements: A systematic review. Gait Posture 2009;29(3):360–9.
27. Hsieh YF, Wang T, Turner CH. Viscoelastic response of the rat loading model: implications for studies of strain-adaptive bone formation. Bone 1999;25(3):379–82.
28. Seth A, Hicks JL, Uchida TK, Habib A, Dembia CL, Dunne JJ, et al. OpenSim: Simulating musculoskeletal dynamics and neuromuscular control to study human and animal movement. PLoS Comput Biol 2018;14(7):e1006223.
29. Delp SL, Anderson FC, Arnold AS, Loan P, Habib A, John CT, et al. OpenSim: Open-Source Software to Create and Analyze Dynamic Simulations of Movement. IEEE Trans Biomed Eng 2007;54(11):1940–50.
30. ANDERSON FC, PANDY MG. A Dynamic Optimization Solution for Vertical Jumping in Three Dimensions. Comput Methods Biomech Biomed Engin 1999; 2(3):201–31.
31. Kawalilak CE, Kontulainen SA, Amini MA, Lanovaz JL, Olszynski WP, Johnston JD. In vivo precision of three HR-pQCT-derived finite element models of the distal radius and tibia in postmenopausal women. BMC Musculoskelet Disord 2016;17(1):389.
32. Pistoia W, van Rietbergen B, Lochmüller EM, Lill CA, Eckstein F, Rüegsegger P. Estimation of distal radius failure load with micro-finite element analysis models based on three-dimensional peripheral quantitative computed tomography images. Bone

2002;30(6):842–8.
33. Holm S. A simple sequentially rejective multiple test procedure. Scand J Statist 1979;6(2):65–70.
34. Aickin M, Gensler H. Adjusting for multiple testing when reporting research results: the Bonferroni vs Holm methods. Am J Public Health 1996;86(5):726–8.
35. Cortes N, Onate J, Abrantes J, Gagen L, Dowling E, Van Lunen B. Effects of Gender and Foot-Landing Techniques on Lower Extremity Kinematics during Drop-Jump Landings. J Appl Biomech 2007;23(4):289–99.
36. Vlachopoulos D, Barker AR, Ubago-Guisado E, Williams CA, Gracia-Marco L. The effect of a high-impact jumping intervention on bone mass, bone stiffness and fitness parameters in adolescent athletes. Arch Osteoporos 2018;13(1):128.
37. Zhao R, Zhao M, Zhang L. Efficiency of Jumping Exercise in Improving Bone Mineral Density Among Premenopausal Women: A Meta-Analysis. Sports Medicine 2014;44(10):1393–402.
38. Nguyen VH. School-based exercise interventions effectively increase bone mineralization in children and adolescents. Osteoporos Sarcopenia 2018;4(2):39–46.
39. Watson SL, Weeks BK, Weis LJ, Harding AT, Horan SA, Beck BR. High-Intensity Resistance and Impact Training Improves Bone Mineral Density and Physical Function in Postmenopausal Women With Osteopenia and Osteoporosis: The LIFTMOR Randomized Controlled Trial. Journal of Bone and Mineral Research 2018;33(2):211–20.
40. Weinhandl JT, Joshi M, O'Connor KM. Gender Comparisons between Unilateral and Bilateral Landings. J Appl Biomech 2010;26(4):444–53.
41. Sara LK, Gaudette LW, Souza Júnior JR de, Tenforde AS, Wasserman L, Johnson CD. Cues to land softly and quietly result in acute reductions in ground reaction force loading rates in runners. Gait Posture 2024;109:220–5.
42. Schmitz RJ, Kulas AS, Perrin DH, Riemann BL, Shultz SJ. Sex differences in lower extremity biomechanics during single leg landings. Clinical Biomechanics 2007;22(6):681–8.
43. Laughlin WA, Weinhandl JT, Kernozek TW, Cobb SC, Keenan KG, O'Connor KM. The effects of single-leg landing technique on ACL loading. J Biomech 2011;44(10):1845–51.
44. Moore IS, Willy RW. Use of Wearables: Tracking and Retraining in Endurance Runners. Curr Sports Med Rep 2019;18(12):437–44.
45. Burt LA, Liang Z, Sajobi TT, Hanley DA, Boyd SK. Sex- and Site-Specific Normative Data Curves for HR-pQCT. Journal of Bone and Mineral Research 2016;31(11):2041–7.
46. Roelker SA, Caruthers EJ, Hall RK, Pelz NC, Chaudhari AMW, Siston RA. Effects of Optimization Technique on Simulated Muscle Activations and Forces. J Appl Biomech 2020;36(4):259–78.
47. MacNeil JA, Boyd SK. Bone strength at the distal radius can be estimated from high-resolution peripheral quantitative computed tomography and the finite element method. Bone 2008;42(6):1203–13.
48. Johnson JE, Troy KL. Validation of a new multiscale finite element analysis approach at the distal radius. Med Eng Phys 2017;44:16–24.

Appendix A: Bivariate Regressions

Table A1. Bivariate regressions of height and landing limbs with each outcome.

Outcomes	β coefficients				MAE (SD)	R^2	Model p-value
	Intercept	Height	Landing Limbs	Interaction			
DIS	6.67	-0.719	2.44	7.33	0.735	0.155	0.135
IMU_FFT	986	205	190	291	0.732	0.149	0.215
RXF	3.64	2.59	-1.03	-0.447	0.568	0.472	<0.001
RXF_R	124	128	-36.9	2.76	0.718	0.084	0.247
RXF_FFT	155	79.1	-45.5	-11.9	0.421	0.704	<0.001
JCF	10.8	12.4	-1.6	-4.24	0.617	0.433	<0.001
JCF_R	194	163	-48.9	-33.5	0.629	0.381	<0.001
JCF_FFT	611	441	-155	-121	0.536	0.537	<0.001
RXF_FE	$8.34*10^{-3}$	$5.17*10^{-3}$	$-2.18*10^{-3}$	$-8.48*10^{-4}$	0.66	0.289	0.002
RXF_FE_FFT	$5.37*10^{-4}$	$3.14*10^{-4}$	$-1.51*10^{-4}$	$-5.16*10^{-5}$	0.64	0.33	0.003
RXF_SMR	1.04	1.77	-0.413	-0.286	0.637	0.110	0.178
JCF_FE	$2.38*10^{-2}$	$2.69*10^{-2}$	$-3.34*10^{-3}$	$-9.10*10^{-3}$	0.628	0.347	<0.001
JCF_FE_FFT	$2.17*10^{-3}$	$1.58*10^{-3}$	$-5.66*10^{-4}$	$-3.69*10^{-4}$	0.650	0.219	0.006
JCF_SMR	4.07	10.8	-1.19	-3.84	0.615	0.380	<0.001

Table A2. Bivariate regressions of sex and height with each outcome.

Outcomes	β coefficients				MAE (SD)	R^2	Model p-value
	Intercept	Sex	Height	Interaction			
DIS	8.59	5.08	13.8	-7.36	0.813	0.029	0.531
IMU_FFT	1190	261	800	-355	0.815	0.010	0.677
RXF	1.56	0.817	2.67	-1.30	0.808	0.085	0.256
RXF_R	39.9	49.9	198	-125	0.746	0.059	0.362
RXF_FFT	73.5	15.5	74.1	-17.2	0.854	0.071	0.373
JCF	8.15	$-6.77*10^{-2}$	5.99	0.197	0.797	0.058	0.358
JCF_R	111	5.30	108	16.6	0.763	0.067	0.367
JCF_FFT	389	-63.6	215	113	0.786	0.036	0.493
RXF_FE	$4.29*10^{-3}$	$8.76*10^{-4}$	$5.57*10^{-3}$	$-2.62*10^{-3}$	0.803	0.025	0.658
RXF_FE_FFT	$3.37*10^{--4}$	$-7.75*10^{-5}$	$3.05*10^{-4}$	$-1.07*10^{--4}$	0.736	0.166	0.051
RXF_SMR	0.189	0.305	2.04	-1.19	0.728	0.006	0.596
JCF_FE	$1.93*10^{-2}$	$-1.71*10^{-3}$	$1.34*10^{-2}$	$-6.01*10^{--4}$	0.780	0.058	0.427
JCF_FE_FFT	$1.66*10^{-3}$	$-7.09*10^{-4}$	$9.39*10^{-4}$	$1.43*10^{--4}$	0.685	0.165	0.123
JCF_SMR	2.33	-0.381	4.51	0.710	0.772	0.016	0.657

Table A3. Bivariate regressions of sex and landing limbs with each outcome.

Outcomes	β coefficients				MAE (SD)	R^2	Model p-value
	Intercept	Sex	Landing Limbs	Interaction			
DIS	4.55	3.82	6.09	-0.977	0.763	0.103	0.279
IMU_FFT	963	229	347	-61.9	0.745	0.126	0.256
RXF	4.89	-0.156	-1.33	0.206	0.591	0.414	<0.001
RXF_R	210	-51.4	-50.808	27.452	0.746	0.027	0.566
RXF_FFT	188	4.91	-51.128	0.018	0.462	0.647	<0.001
JCF	17.12	-1.31	-3.921	0.723	0.661	0.337	<0.001
JCF_R	273	-11.96	-70.853	13.368	0.653	0.316	<0.001
JCF_FFT	843	-58.67	-223.128	21.570	0.563	0.480	<0.001
RXF_FE	$1.14*10^{-2}$	$-1.10*10^{-3}$	$-2.84*10^{-3}$	$3.91*10^{-4}$	0.688	0.256	0.041
RXF_FE_FFT	$8.16*10^{-4}$	$-2.21*10^{-4}$	$-2.12*10^{-4}$	$5.27*10^{-5}$	0.546	0.520	<0.001
RXF_SMR	2.33	-0.821	-0.758	0.347	0.660	0.073	0.459
JCF_FE	$3.94*10^{-2}$	$-5.53*10^{-3}$	$-8.76*10^{-3}$	$1.93*10^{-3}$	0.669	0.289	0.001
JCF_FE_FFT	$3.63*10^{-3}$	$-1.21*10^{-3}$	$-9.57*10^{-4}$	$3.25*10^{-4}$	0.553	0.426	<0.001
JCF_SMR	9.89	-1.58	-3.438	0.837	0.631	0.308	<0.001

Appendix B. Linear Regression with LASSO

Table B1. Average testing results after five-fold cross validation using height, landing limbs, sex, and kinematics to model each outcome.

Outcomes	mean	Standard deviation	Average testing MAE (SD)	Total Model r^2	Model p-value
DIS	15.35	7.25	0.59	0.41	$1.86*10^{-2}$
IMU_FFT	1580.18	408.39	0.58	0.43	$1.18*10^{-2}$
RXF	2.87	0.96	0.53	0.52	<0.001
RXF_R	125.52	71.20	0.68	0.10	0.70
RXF_FFT	110.42	31.32	0.40	0.73	<0.001
JCF	10.84	2.89	0.49	0.65	<0.001
JCF_R	165.85	54.68	0.45	0.72	<0.001
JCF_FFT	479.07	149.25	0.42	0.72	<0.001
RXF_FE	$6.65*10^{-3}$	$2.49*10^{-3}$	0.57	0.43	$1.90*10^{-4}$
RXF_FE_FFT	$4.08*10^{-4}$	$1.53*10^{-4}$	0.46	0.60	<0.001
RXF_SMR	0.99	0.91	0.60	0.15	0.45
JCF_FE	$2.43*10^{-2}$	$6.81*10^{-3}$	0.38	0.76	<0.001
JCF_FE_FFT	$1.74*10^{-3}$	$7.54*10^{-4}$	0.48	0.62	<0.001
JCF_SMR	4.33	2.55	0.42	0.72	<0.001

Table B2. Average coefficients after five-fold cross validation using height, landing limbs, sex, and kinematics to model each outcome.

Outcomes	β Coefficients								
	Height	Landing Limbs	Sex	Hip Flexion ROM	Knee Flexion ROM	Ankle Flexion ROM	Hip Flexion at Contact	Knee Flexion at Contact	Ankle Flexion at Contact
DIS	1.25	2.60	1.18	-0.36	1.94	-2.11	0.61	3.00	2.15
IMU_FFT	68.84	133.12	66.16	-26.32	130.33	-119.18	21.59	139.71	102.26
RXF	0.35	-0.50	$4.10*10^{-2}$	-0.11	-0.14	0.12	-0.15	$7.84*10^{-2}$	0.15
RXF_R	21.19	-12.92	-2.55	-7.96	-0.56	5.31	-7.59	5.65	3.83
RXF_FFT	9.05	-23.81	1.80	-2.60	-0.27	1.72	-3.13	0.27	2.17
JCF	0.58	-1.74	$2.60*10^{-2}$	$-5.99*10^{-2}$	$-1.95*10^{-2}$	1.13	-0.15	-0.19	$8.38*10^{-2}$
JCF_R	16.12	-27.67	4.44	2.77	-13.37	20.06	-10.10	-7.79	1.81
JCF_FFT	19.86	-105.53	-1.55	-3.22	3.04	52.87	-0.45	-14.06	0.23
RXF_FE	9.79*10-4	$-7.08*10^{-4}$	$-4.37*10^{-4}$	$-3.10*10^{-4}$	$-9.60*10^{-4}$	$5.15*10^{-4}$	$-3.12*10^{-4}$	$1.56*10^{-4}$	$3.47*10^{-4}$
RXF_FE_FFT	$4.59*10^{-5}$	$-6.97*10^{-5}$	$-7.42*10^{-5}$	$-8.51*10^{-6}$	$-3.25*10^{-5}$	$3.07*10^{-5}$	$-2.17*10^{-5}$	$1.37*10^{-5}$	$1.28*10^{-5}$
RXF_SMR	0.26	-0.15	-0.17	-0.17	$-8.18*10^{-2}$	$7.26*10^{-2}$	$-7.74*10^{-2}$	$9.21*10^{-2}$	$5.49*10^{-2}$
JCF_FE	$1.74*10^{-3}$	$-2.84*10^{-3}$	$-9.51*10^{-4}$	$7.25*10^{-5}$	$-2.37*10^{-3}$	$3.93*10^{-3}$	$-1.77*10^{-4}$	$-9.20*10^{-4}$	$2.34*10^{-4}$
JCF_FE_FFT	$9.84*10^{-5}$	$-3.32*10^{-4}$	$-3.03*10^{-4}$	$2.08*10^{-5}$	$-1.28*10^{-4}$	$3.60*10^{-5}$	$-3.43*10^{-5}$	$-5.42*10^{-5}$	$-2.50*10^{-5}$
JCF_SMR	0.56	-1.28	$-5.61*10^{-2}$	0.14	-0.57	1.21	-0.33	-0.46	$-2.00*10^{-2}$

**ROM = Range Of Motion.*

Table B3. Average coefficient p-values after five-fold cross validation using height, landing limbs, sex, and kinematics to model each outcome.

Outcomes	β Coefficient p-values								
	Height	Landing Limbs	Sex	Hip Flexion ROM	Knee Flexion ROM	Ankle Flexion ROM	Hip Flexion at Contact	Knee Flexion at Contact	Ankle Flexion at Contact
DIS	0.52	0.13	0.54	0.70	0.42	0.11	0.62	0.21	0.34
IMU_FFT	0.54	0.16	0.53	0.67	0.35	0.11	0.85	0.30	0.41
RXF	0.11	0.01	0.75	0.45	0.42	0.26	0.18	0.59	0.37
RXF_R	0.19	0.39	0.81	0.55	0.98	0.54	0.43	0.67	0.89
RXF_FFT	0.10	<0.01	0.53	0.45	0.97	0.45	0.21	0.96	0.53
JCF	0.18	<0.01	0.92	0.77	0.98	<0.01	0.54	0.62	0.72
JCF_R	0.11	<0.01	0.45	0.65	0.22	0.01	0.11	0.41	0.70
JCF_FFT	0.28	<0.01	0.93	0.75	0.77	<0.01	0.87	0.49	0.99
RXF_FE	0.12	0.11	0.20	0.50	0.11	0.12	0.32	0.65	0.42
RXF_FE_FFT	0.12	0.01	<0.01	0.65	0.26	0.07	0.19	0.53	0.53
RXF_SMR	0.22	0.43	0.26	0.43	0.63	0.56	0.51	0.60	0.68
JCF_FE	0.13	<0.01	0.19	0.92	0.07	<0.01	0.70	0.37	0.75
JCF_FE_FFT	0.33	0.01	<0.01	0.69	0.34	<0.01	0.58	0.59	0.70
JCF_SMR	0.18	0.00	0.86	0.81	0.25	<0.01	0.24	0.30	0.85

**ROM = Range Of Motion*

Table B4. Average testing results after five-fold cross validation using height, landing limbs, sex, kinematics, and reaction forces to model each outcome.

Outcomes	mean	Standard deviation	Average testing MAE (SD)	Total Model r^2	Model p-value
RXF_FE	$6.65*10^{-3}$	$2.49*10^{-3}$	0.30	0.86	<0.001
RXF_FE_FFT	$4.08*10^{-4}$	$1.53*10^{-4}$	0.30	0.86	<0.001
RXF_SMR	0.99	0.91	0.18	0.93	<0.001
JCF_FE	$2.43*10^{-2}$	$6.81*10^{-3}$	0.36	0.79	<0.001
JCF_FE_FFT	$1.74*10^{-3}$	$7.54*10^{-4}$	0.48	0.64	<0.001
JCF_SMR	4.33	2.55	0.38	0.78	<0.001

Table B5. Average coefficients after five-fold cross validation using height, landing limbs, sex, kinematics, and reaction forces to model each outcome.

β Coefficients	Outcomes					
	RXF_FE	RXF_FE_FFT	RXF_SMR	JCF_FE	JCF_FE_FFT	JCF_SMR
Height	$1.68*10^{-4}$	$1.03*10^{-5}$	$1.50*10^{-3}$	$1.25*10^{-3}$	$5.91*10^{-5}$	0.223
Landing Limbs	$2.67*10^{-4}$	$1.43*10^{-5}$	$2.72*10^{-3}$	$-7.19*10^{-5}$	$-6.28*10^{-5}$	0.276
Sex	$-3.24*10^{-4}$	$-7.17*10^{-5}$	$-6.64*10^{-2}$	$-1.39*10^{-3}$	$-3.36*10^{-4}$	-0.268
Hip Flexion ROM	$-1.83*10^{-5}$	$5.68*10^{-6}$	$-3.09*10^{-2}$	$8.05*10^{-5}$	$2.58*10^{-5}$	0.184
Knee Flexion ROM	$-6.04*10^{-4}$	$-3.36*10^{-5}$	$-2.34*10^{-2}$	$-2.34*10^{-3}$	$-1.54*10^{-4}$	-0.505
Ankle Flexion ROM	$2.81*10^{-4}$	$2.53*10^{-5}$	$1.21*10^{-2}$	$3.80*10^{-3}$	$3.57*10^{-4}$	1.13
Hip Flexion at Contact	$3.16*10^{-5}$	$-8.91*10^{-6}$	$1.43*10^{-2}$	$-2.50*10^{-5}$	$-3.40*10^{-5}$	-0.184
Knee Flexion at Contact	$-7.36*10^{-5}$	$6.77*10^{-6}$	$-4.87*10^{-3}$	$-5.71*10^{-4}$	$-4.65*10^{-5}$	-0.303
Ankle Flexion at Contact	$2.61*10^{-5}$	$1.07*10^{-6}$	$-6.56*10^{-3}$	$2.22*10^{-4}$	$-3.70*10^{-5}$	$-8.02*10^{-2}$
RXF	$1.40*10^{-3}$	$-2.88*10^{-5}$	0.138	$3.56*10^{-4}$	$-1.65*10^{-4}$	0.596
RXF_R	$4.98*10^{-4}$	$3.29*10^{-5}$	0.722	$-2.27*10^{-3}$	$-1.05*10^{-4}$	-1.34
RXF_FFT	$3.31*10^{-4}$	$1.22*10^{-4}$	0	$3.79*10^{-3}$	$4.82*10^{-4}$	1.90
*ROM = Range Of Motion						

Table B6. Average coefficient p-values after five-fold cross validation using height, landing limbs, sex, kinematics, and reaction forces to model each outcome.

β Coefficient p-values	Outcomes					
	RXF_FE	RXF_FE_FFT	RXF_SMR	JCF_FE	JCF_FE_FFT	JCF_SMR
Height	0.52	0.50	0.99	0.25	0.62	0.57
Landing Limbs	0.65	0.62	0.99	0.94	0.82	0.66
Sex	0.12	<0.01	0.24	0.07	<0.01	0.35
Hip Flexion ROM	0.90	0.63	0.61	0.95	0.71	0.58
Knee Flexion ROM	0.08	0.09	0.73	0.07	0.28	0.28
Ankle Flexion ROM	0.11	0.02	0.86	<0.01	<0.01	**<0.01**
Hip Flexion at Contact	0.89	0.36	0.82	0.93	0.60	0.46
Knee Flexion at Contact	0.68	0.59	0.97	0.52	0.62	0.44
Ankle Flexion at Contact	0.93	0.74	0.95	0.78	0.64	0.66
RXF	0.01	0.38	0.36	0.85	0.49	0.45
RXF_R	0.13	0.09	<0.01	0.08	0.43	0.01
RXF_FFT	0.73	0.01	1	0.16	0.18	0.11
*ROM = Range Of Motion						

Table B7. Average testing results after five-fold cross validation using height, landing limbs, sex, kinematics, and reaction forces to model each outcome.

Outcomes	mean	Standard deviation	Average testing MAE (SD)	Total Model r^2	Model p-value
JCF_FE	$2.43*10^{-2}$	$6.81*10^{-3}$	0.29	0.86	<0.001
JCF_FE_FFT	$1.74*10^{-3}$	$7.54*10^{-4}$	0.24	0.90	<0.001
JCF_SMR	4.33	2.55	0.18	0.95	<0.001

Table B8. Average coefficients after five-fold cross validation using height, landing limbs, sex, kinematics, reaction and contact forces model each outcome.

β Coefficients	Outcomes		
	JCF_FE	JCF_FE_FFT	JCF_SMR
Height	$8.85*10^{-4}$	$6.71*10^{-5}$	$3.79*10^{-3}$
Landing Limbs	$5.59*10^{-4}$	$6.17*10^{-5}$	0.983
Sex	$-1.17*10^{-3}$	$-3.01*10^{-4}$	-0.174
Hip Flexion ROM	$1.03*10^{-4}$	$8.77*10^{-5}$	0.169
Knee Flexion ROM	$-2.40*10^{-3}$	$-2.42*10^{-4}$	-0.356
Ankle Flexion ROM	$2.12*10^{-3}$	$1.66*10^{-4}$	0.292
Hip Flexion at Contact	$7.48*10^{-5}$	$-5.73*10^{-5}$	$-1.88*10^{-2}$
Knee Flexion at Contact	$-6.49*10^{-5}$	$3.25*10^{-5}$	$7.72*10^{-3}$
Ankle Flexion at Contact	$4.57*10^{-4}$	$1.26*10^{-5}$	$3.62*10^{-2}$
RXF	$-2.36*10^{-4}$	$-2.51*10^{-5}$	$-7.27*10^{-2}$
RXF_R	$-3.28*10^{-5}$	$9.69*10^{-5}$	$5.45*10^{-2}$
RXF_FFT	$7.58*10^{-4}$	$-8.62*10^{-5}$	0.158
JCF	$2.77*10^{-3}$	$-2.45*10^{-4}$	0.413
JCF_R	$-4.42*10^{-6}$	$-1.84*10^{-5}$	1.36
JCF_FFT	$1.69*10^{-3}$	$8.23*10^{-4}$	0.604
*ROM = Range Of Motion			

Table B9. Average coefficient p-values after five-fold cross validation using height, landing limbs, sex, kinematics, reaction and contact forces to model each outcome.

β Coefficient p-values	Outcomes		
	JCF_FE	JCF_FE_FFT	JCF_SMR
Height	0.30	0.36	0.98
Landing Limbs	0.74	0.64	0.55
Sex	0.07	<0.01	0.21
Hip Flexion ROM	0.76	0.25	0.36
Knee Flexion ROM	0.03	0.02	0.19
Ankle Flexion ROM	<0.01	<0.01	<0.01
Hip Flexion at Contact	0.76	0.26	0.84
Knee Flexion at Contact	0.79	0.58	0.96
Ankle Flexion at Contact	0.48	0.76	0.79
RXF	0.92	0.88	0.89
RXF_R	0.76	0.30	0.70
RXF_FFT	0.82	0.59	0.83
JCF	0.65	0.56	0.20
JCF_R	0.98	0.60	<0.01
JCF_FFT	0.15	<0.01	0.04
*ROM = Range Of Motion			